

Aggregate shape influence on the fracture behaviour of concrete

N. Monteiro Azevedo[†]

Faculdade de Ciências e Tecnologia, Universidade Nova de Lisboa, Portugal

J. V. Lemos[‡]

LNEC, Av. Brasil 101, 1700-066 Lisboa, Portugal

(Received October 7, 2005, Accepted June 20, 2006)

Abstract. The Discrete Element Method, DEM, is increasingly used in fracture studies of non-homogeneous continuous media, such as rock and concrete. A 2D circular rigid DEM formulation, developed to model concrete, has been adopted. A procedure developed to generate aggregate particles with a given aspect ratio and shape is presented. The aggregate particles are modelled with macro-particles formed by a group of circular particles that behave as a rigid body. Uniaxial tensile and compression tests performed with circular and non-circular aggregates, with a given aspect ratio, have shown similar values of fracture toughness when adopting uniform strength and elastic properties for all the contacts. Non-circular aggregate assemblies are shown to have higher fracture toughness when different strength and elastic properties are set for the matrix and for the aggregate/matrix contacts.

Keywords: particle methods; discrete element; aggregate shape; concrete fracture.

1. Introduction

A numerical model of concrete under short-term loading should embody a suitable procedure to deal with the formation and propagation of cracks and their effects on the overall behaviour of concrete based structures. The complex constitutive behaviour arising from extensive micro-cracking and macro-cracking is difficult to characterize in terms of a continuum formulation. An appropriate stress-strain law for the material may not exist or the law may be excessively complicated.

Particle models taking directly into consideration the physical mechanisms and the influence of the concrete aggregate-structure have been developed to model fracture in concrete. Contrary to continuum formulations the development of cracks and ruptures surfaces is well handled by particle models. By simulating the concrete aggregate-structure a particle method prevents the localization of damage into regions not sufficiently large when compared to the inhomogeneity size, Bazant (1986).

[†] Auxiliar Professor, Corresponding author, Laboratório Nacional de Engenharia Civil (LNEC), Portugal
E-mail: nazevedo@lnec.pt

[‡] E-mail: vlemos@lnec.pt

The first particle models were the so-called lattice models that have been inspired in the work of Hrennikoff (1941), which introduced a regular triangular network of truss members to solve classical problems of elasticity, and in the work of theoretical physicists that have used it to analyse conductivity problems and to model brittle failure in disordered materials, Herrmann *et al.* (1989).

Lattice models have also been proposed as a micromechanical model to study fracture process in heterogeneous materials, Schlangen *et al.* (1996). In the lattice model the material is discretized using one-dimensional elements (e.g., a spring network, a spring network with shear elements, or a spring network with shear and bending elements) that allow force transfer between the nodes forming the lattice. Fracture simulation is carried out by performing a linear elastic analysis, on each load step, the element within the mesh that exceeds a given threshold value by the largest amount is removed.

The Discrete Element Method, DEM, was initially introduced for the study of discontinuous rock. Rigid circular particle models have also been developed for the study of the micro-mechanic behaviour of soils, Cundall and Strack (1979). Recently, circular particle models have also been applied in the study of fracture analysis in rock, Potyondy and Cundall (1996), and concrete, Meguro and Hakuno (1989) and Takada and Hassani (1996). This has been accomplished through the development of constitutive models for the inter-particle contacts enabling the geo-materials modelling.

When compared to particle models based on lattice methods, which have been developed to study fracture mechanisms of quasi-brittle material, the DEM based particle model allows high particle displacements and rotations which are relevant at the aggregate-scale namely on assemblies under compression, where the particle displacements are close to the aggregate size scale. Also with DEM the inter-particle stiffness matrix has a physical meaning given by contact interaction, and the solution scheme is based on an explicit time marching scheme following the particle assembly evolution step by step allowing crack formation to dynamically influence and disturb neighbouring particles in real time.

Recently, a 2D and a 3D formulation for a discrete element spherical particle model developed for Rock fracture studies has been proposed, Potyondy and Cundall (2004). The model has been shown to reproduce many features of rock behaviour, including elasticity, dilation, post-peak behaviour, fracturing, acoustic emission, post-peak softening and strength increase with confinement. All this macroscopic behaviours are emergent properties of the DEM model that arise given the particle assembly and a relatively simple set of micro-properties.

In the approach here adopted, concrete is regarded as a skeleton of aggregate particles of various sizes, almost in direct contact with each other. The cement matrix is intended to act as filler enabling the structure to be able to carry tensile stresses. A 2D rigid circular particle model based on the DEM that has been developed to model concrete fracture has been adopted (Monteiro Azevedo 2003). This particle model was shown to give a good agreement with concrete experimental data, namely the peak stress values, the crack initiation and crack localization (Monteiro Azevedo *et al.* 2003).

In Jensen *et al.* (1999) macro-particles given as a group of smaller particles working as a rigid body are shown to undergo less rolling and provide increased shear strength. In Monteiro Azevedo (2003) macro-particles are also shown to increase the fracture toughness of the particle assembly. In both works, the adopted macro-particles have a reduced number of circular particles forming it, so the particle shape and aspect ratio are not so accurately defined.

Before applying the particle model it is required to previously generate a particle assembly based

on a given aggregate sieve analysis, in a manner similar to the generation of a mesh when using a finite element method. Recently, particle generation algorithms have been proposed that enable the generation of an aggregate particle structure that follows the shape, the size, the aspect ratio and the distribution of the aggregate particles present in concrete (Monteiro Azevedo and Lemos 2003). The proposed particle generation algorithms include both the generation of all-circular particle assemblies or hybrid assemblies with circular and polygonal particles. It is important to point out that that one can create a polygonal particle formed by a cluster of smaller circular particles within its boundary.

Even though some researchers have currently developed 3D particle DEM or lattice models, Potyondy and Cundall (2004), Hentz *et al.* (2004) and Cusatis *et al.* (2003), the development of current 2D models should still be carried out. When compared to 3D models, the 2D models can be easily applied in more complex geometries and in higher scales given the fact that the 3D models require a much higher number of particles leading to an extremely higher computational cost. Also, the improvements in the particle generation here referred are easily transferred to 3D, and the extensions to a particle model should be first tested and matured on a 2D model and after extended to 3D.

The behaviour of the adopted 2D discrete model enhanced with the new particle generation scheme has been assessed in uniaxial tension and compression tests. The influence of the particle geometry and the particle elongation ratio of the particles representing the concrete aggregates have been evaluated. With particle models one should try to mimic the aggregate content as it is present in concrete.

The numerical results are compared to the results obtained numerically by Vonk (1993) which are known to agree with experimental data. Vonk uses a micromechanical approach based on the distinct element method adopting deformable polygonal elements, Cundall (1980).

2. Formulation

In the DEM the domain is replaced with an assembly of discrete entities that interact with each other through contact points or contact interfaces. As proposed by Cundall and Strack (1992) in order for an algorithm to be defined as DEM it has to allow finite displacements and rotations of the discrete bodies, including complete detachment. It also has to be able to recognize new contacts as the calculation progresses.

In the DEM the set of forces acting on each block/particle are related to the relative displacement of the block/particle with respect to its neighbours. Given the applied forces, Newton's 2nd law of motion is applied in order to define the new position of the block/particle. The relation between the generalized forces transmitted through the contact and applied at the centre of gravity of the particles to the generalized displacements at the centre of gravity of the particles, see Fig. 1, can be expressed by:

$$\{f\} = [K^e]\{d\} \quad (1)$$

where, $\{f\}$ is the generalized force vector, $\{d\}$ is the generalized displacement vector and $[K^e]$ is the contact stiffness matrix in terms of particle displacements. As shown in Fig. 1, each particle has six degrees of freedom and the interaction between them is made at the contact point, the mid-point of the line connecting the particles centre of gravity, through a normal and a shear spring.

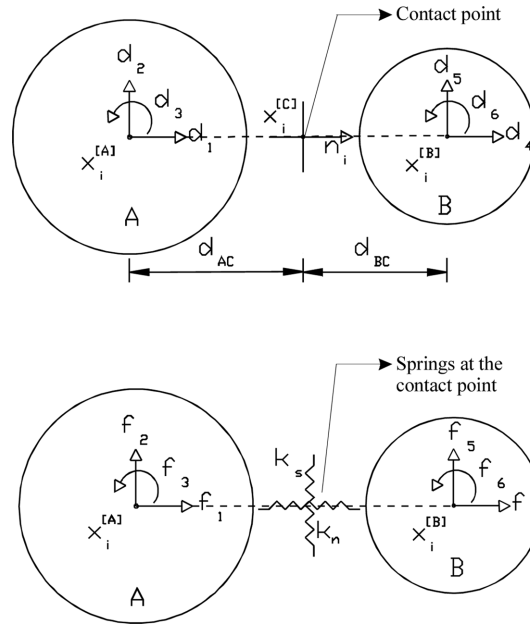


Fig. 1 Forces and displacements for a given contact

The generalized force and displacement vectors are given, in accordance with Fig. 1, by:

$$\{f\} = \{f_1, f_2, f_3, f_4, f_5, f_6\}^t, \quad \{d\} = \{d_1, d_2, d_3, d_4, d_5, d_6\}^t \quad (2)$$

The single contact element stiffness matrix, $[K^e]$, in terms of particle displacements for a reference plane passing through the normal to the point contact $n_i = (n_1, n_2)$ is defined by:

$$\begin{bmatrix} k_n & 0 & 0 & -k_n & 0 & 0 \\ 0 & k_s & d_{AC}k_s & 0 & -k_s & d_{BC}k_s \\ 0 & d_{AC}k_s & d_{AC}^2k_s & 0 & -d_{AC}k_s & d_{AC}d_{BC}k_s \\ -k_n & 0 & 0 & k_n & 0 & 0 \\ 0 & -k_s & -d_{AC}k_s & 0 & k_s & -d_{BC}k_s \\ 0 & d_{BC}k_s & d_{AC}d_{BC}k_s & 0 & -d_{BC}k_s & d_{BC}^2k_s \end{bmatrix} \quad (3)$$

where, k_n and k_s are the contact normal and shear stiffness; $d_A = \|x_i^{[A]} - x_i^{[C]}\|$ and $d_B = \|x_i^{[B]} - x_i^{[C]}\|$ are the Euclidean norm of the corresponding vectors; $x_i^{[A]}$ and $x_i^{[B]}$ are the centres of gravity of particles A and B , respectively and $x_i^{[C]}$ represents the contact point coordinates.

An explicit time marching calculation scheme based on the centred-difference algorithm is adopted. At each time step the local stiffness matrix is evaluated and the contact normal direction is updated. Then the particle forces are calculated given the inter-particle displacement increments.

The total translation stiffness k_t and the rotational stiffness k_θ of each particle must include, for a given time step, the contribution of all the particles in contact:

$$k_t = \sum_{c=1}^{N_c} 2(k_{n,c} + k_{s,c}) \quad (4)$$

$$k_\theta = \sum_{c=1}^{N_c} (d_{BC}^2 k_{s,c} + d_{AC} d_{BC} k_{s,c}) \quad (5)$$

where N_c is the number of particles in contact with the given particle. The contact stiffnesses are defined using:

$$k_n = \frac{E' h}{L} t; \quad k_s = \frac{E'' h}{L} t \quad (6)$$

where, L is the inter-particle distance, t is the thickness of the particle assembly, h is defined as the contact height, being equal to the smallest diameter of the particles involved, and for plane stress:

$$E' = \frac{E}{1 - \nu^2} \quad \text{and} \quad E'' = \frac{E}{2(1 + \nu)} \quad (7)$$

where, E and ν are the Young's modulus and the Poisson's ratio of the continuum material.

Eq. (6) establishes a simple relationship between macro and micro responses that consider the inter-particle size, and can be devised as the axial and shear stiffness of the equivalent continuum of two particles in interaction, see Fig. 2.

When only a steady state solution is sought, a density scaling algorithm is adopted in order to reduce the number of time steps necessary to reach the desired solution, Underwood (1983). With this algorithm the particles mass and inertia are artificially scaled so the centred-difference algorithm has a higher rate of convergence for a given loading step. The particle scaled mass and scaled inertia used in the calculations are then set given the particle stiffness at a given time increment through:

$$m^{scaled} = 0.25 k_t; \quad I^{scaled} = 0.25 k_\theta \quad (8)$$

In the determination of the contact strength an analogy to the method used in the definition of the contact stiffness is used. The contact strength is set given a simplistic analysis of the equivalent continuum, Fig. 2. The contact strength can then be approximated by:

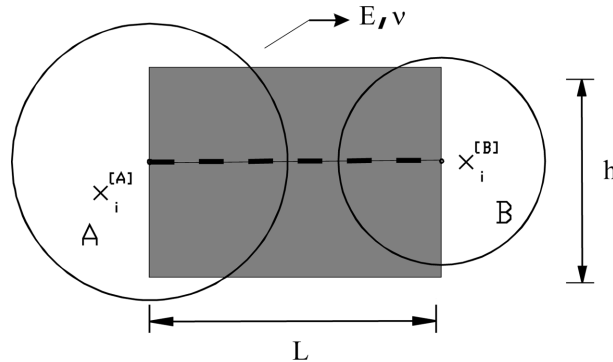


Fig. 2 Equivalent elastic continuum

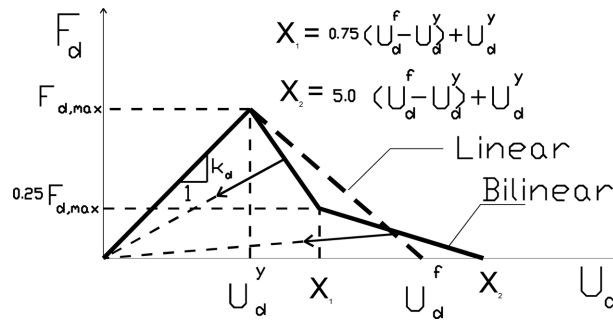


Fig. 3 Contact constitutive laws

$$F_{n,t} = \sigma_{n,t} 2.0 R^{\min} t \quad (9)$$

where, $F_{n,t}$ is the generalized ultimate contact force, $\sigma_{n,t}$ is the ultimate value of the stress in the desired direction, normal or tangent to the contact plane and R^{\min} is the minimum radius of the particles in contact.

For the inter-particle contacts an extended Mohr-Coulomb model with bilinear softening is adopted, Fig. 3. The bilinear softening diagram is based on the model proposed by Rokugo (1989). Given the adopted fracture energy, representing just the area of the softening part of the diagram, the displacement U_d^f is determined. This would be the value of the maximum displacement if one would adopt a simple linear softening diagram, Fig. 3. Then the bilinear diagram is set given the expressions defined in Fig. 3, namely the two points which are required to set a complete a bilinear diagram. As shown in Fig. 3, when compared to the linear diagram, the bilinear gives a lower resistant force at the beginning of the softening behaviour and allows the particles to interact at a higher distance. The maximum contact strength, $F_{d,max}$, is directly defined through Eq. (9).

As the calculation progresses the values of the maximum resistant tensile force and maximum cohesion force are reduced as a function of the current value of the contact damage, which is set given the current inter-particle displacement. Contrary to continuum methods, the softening energy is not related to the macroscopic energy of concrete. Fig. 3 also shows that a secant contact stiffness approach is adopted, for this reason the contact stiffness value is also reduced according to the current value of contact damage.

In the 2D model, the softening energy is considered to be an indirect way to include effects from the 3rd dimension, and to indirectly account for the effects of the aggregate particle grading, the influence of the particle refinement and the grading of the particles representing the cement paste.

To point out that more complex criteria can be considered which set the strength and elastic micro-properties to the known macro properties of the material in analysis, namely the Young modulus, Poisson's ratio, ultimate strength and fracture toughness, Potyondy and Cundall (2004).

3. Particle generation

The modelling of a given structure with the particle method requires the previous definition of the particle distribution based on a given sieve analysis. In Monteiro Azevedo and Lemos (2003)

particle generation algorithms are proposed which allow the generation of compact particles assemblies with the shape, aspect ratio and distribution of the aggregate particles present in concrete.

3.1 Low porosity aggregate structure

The aggregate structure with a low porosity follows the algorithm proposed in Bazant *et al.* (1990):

1 - The volume ratio of each particle size is specified in advance setting the area of aggregate for each adopted grading segment, D_{\min} and D_{\max} , which are, respectively, the maximum and the minimum diameter of a given grading segment.

2 - A given particle diameter is defined using, $D = D_{\min} + \eta_i D_{\max}$, in which η_i is a random number uniformly distributed between 0 and 1.

3 - A uniform probability distribution is assumed for the particles centre of gravity. Under this assumption a random number generator from a standard computer library is used to generate the pairs of coordinates (x_i, y_i) of the particle centres: $x_i = X_{\min} + \eta_1 (X_{\max} - X_{\min})$ and $y_i = Y_{\min} + \eta_2 (Y_{\max} - Y_{\min})$. Where: X_{\min} , X_{\max} , Y_{\min} , Y_{\max} are the minimum and the maximum X - Y coordinates of the rectangular area in consideration, being η_1 and η_2 two independent random numbers uniformly distributed between 0 and 1. Non-rectangular specimens, namely circular specimens need to be previously discretized with bounding rectangular elements. At the end of the generation process the particles outside the real geometry are filtered.

4 - For each generated coordinate pair the new particle is checked for possible overlaps with the previously placed particles and with the specimen boundaries. The coordinate pair is rejected if an overlap occurs. The minimum gap between two particles is taken as a function of the minimum particle diameter of the particles in contact, $\gamma \min(D_A, D_B)$. A value of $\gamma = 0.30$ is suggested in Wang *et al.* (1999). If necessary, the value of γ can be further reduced so all particles can be placed into the domain. A minimum gap of γD_A is adopted for the intersection between the particle and the boundary segment.

5 - The random generation of the coordinate pairs for a given grading segment proceeds until the area of aggregate left to be generated is less than πD_{\min}^2 . The remaining aggregate area to be generated is then transferred to the next grading segment. Particles are first inserted from the grading segment with the highest maximum diameter to the grading segment with the smallest maximum diameter. The procedure is stopped after the last particle of the smallest grading segment is inserted.

For the polygonal particle generation, Wang *et al.* (1999), it is further required to define the particle shape, particle elongation ratio and particle orientation before step 4. The number of vertices of the polygonal particle is a random variable varying uniformly from 4 to 10 vertices. Given the grading segment diameter D the radius of each vertex R_i is given by $R_i = (D/2) + \eta_j \delta(D/2)$, where η_j is a random number uniformly distributed between 0 and 1, $\delta(D/2)$ is the aggregate radius amplitude, a value of 0.25 of the grading segment radius is adopted.

Figs. 7(a) and 7(b) present the aggregate structure adopting, respectively, circular shape and polygonal shape with a variable 1 to 2 aspect ratio. As shown, the random aggregate particle assemblies have a high porosity without real particle contacts. In order to apply the DEM it is necessary to replace the domain of analysis with a particle assembly with a low porosity.

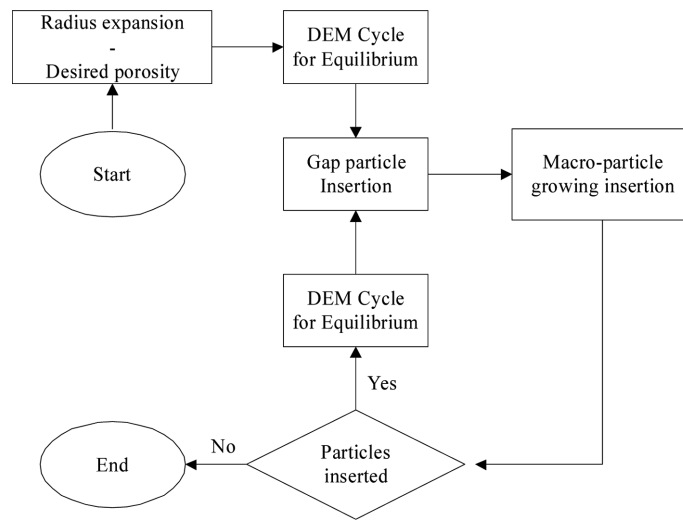


Fig. 4 Void elimination procedure diagram

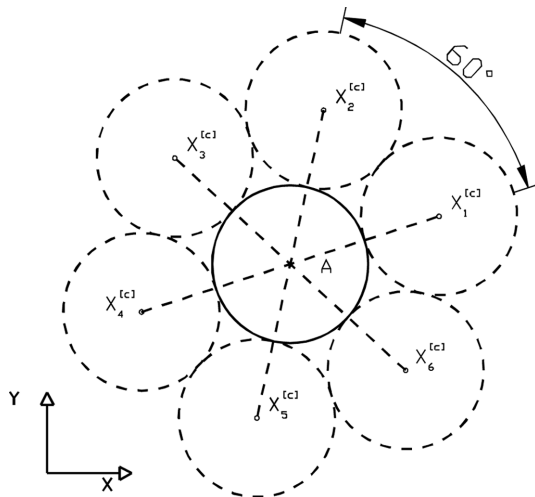


Fig. 5 RMPG six propagation directions

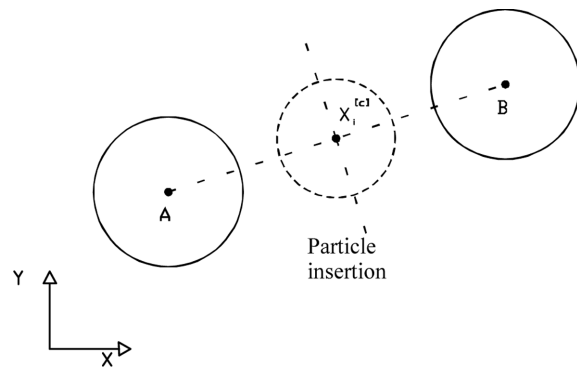


Fig. 6 Gap particle insertion attempt

3.2 Compact assembly

Starting from a low porosity aggregate assembly, a compact particle system is generated according to a void elimination scheme proposed by Monteiro Azevedo (2003) that adopts the DEM in the modelling of the discontinuous behaviour proper of a granular media. The void elimination procedure combines the radius expansion procedure Itasca (1995), the random macro-particle growing procedure Sakaguchi and Mühlhaus (1997), the gap particle insertion mechanism, Monteiro Azevedo (2003) and the DEM cycle, Fig. 4.

The radius expansion procedure places particles based on a given uniform radius grading with half their radius. After the particle placement, the real particle radius is set and the DEM cycle is applied in order to obtain a particle assembly with smaller particle overlaps.

In the random macro-particle growing RMPG procedure algorithm seed particles, SP, positioned on a given domain have six directions of propagation into which new particles can be placed, Fig. 5. A seed particle can be any particle present in the assembly resulting from a radius expansion procedure. A specific direction of propagation is ruled out if the corresponding position has already been occupied by a given particle. The generated particles are not allowed to overlap and they all have the same radius. The directions of propagation are randomly selected.

In a DEM solution cycle a contact detection procedure is applied in order to identify the particles in contact. In order to reduce the contact detection computational costs an enlarged bounding box is usually adopted, Monteiro Azevedo (2003). All the particles that intersect the particle enlarged bounding box are recognized as potential contactors. In the gap particle insertion mechanism, Fig. 6, attempts are made to place particles in the contact location of particles with a gap higher than a certain threshold value taken advantage of the information stored in a DEM program.

Table 1 presents the aggregate content that is taken into consideration when generating the particle assemblies here discussed. The particle assemblies are generated for an area of 100 by 50 mm. On all particle systems a minimum value for the aggregate diameter of 2.00 mm is adopted.

As shown in Figs. 7(a) and 7(b), the concrete aggregate structure with low porosity is first generated given the aggregate content. For the particle assemblies here discussed a minimum distance equal to 0.10 of the minimum radius of the particles in contact is adopted.

The interior domain of each aggregate particle is first discretized, Figs. 7(c) and 7(d) using the void elimination algorithm presented in Fig. 4, with a minimum value of 2.0 mm for the circular particles to be inserted. For circular aggregates an artificial exterior boundary made of small circular particles is created. For the polygonal aggregates the boundary is formed by creating rigid segments connecting the vertices adopting a rigid wall/circular particle contact algorithm as described in

Table 1 Aggregate grading

Aggregate Diam. [mm]	2.00	2.00-4.00	4.00-8.00	8.00-16.00
1879 kg/m ³	42%	14%	20%	24%

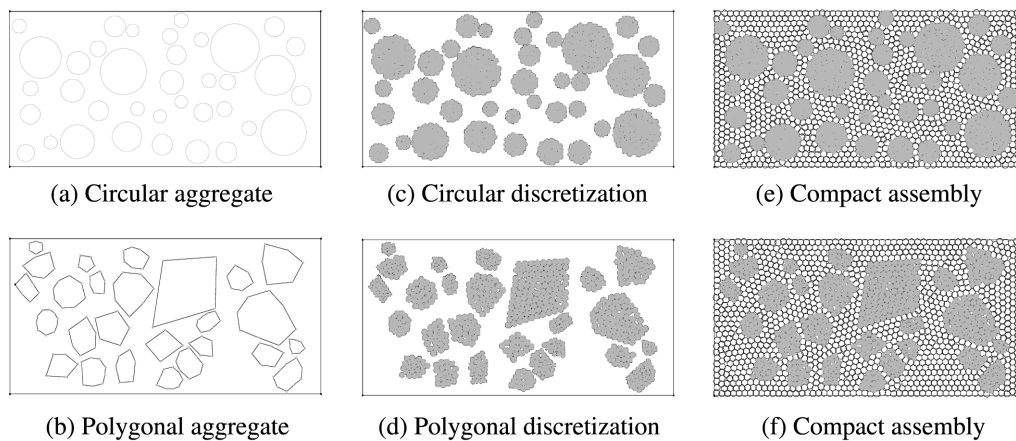


Fig. 7 Particle assemblies – From the aggregate structure to the final compact assembly

Itasca (1995). These boundaries are then discarded after creating a compact assembly of circular particles inside each aggregate particle.

Figs. 7(e) and 7(f) show the final compact assemblies with small circular particles both inside and outside the aggregate particles shown in Figs. 7(a) and 7(b). A clump logic algorithm, Itasca (1995), is adopted for the particle clusters representing the aggregate. For this reason, the particles belonging to the same aggregate particle do not need to be considered to interact, reducing the number of contacts present in the particle assemblies. On each time step all the forces of the particles representing the rigid aggregate are evaluated at the centre of gravity of the aggregate. Newton's 2nd law of motion is defined for the rigid aggregate. The movement of the interior particles forming the aggregate particle is set given the rigid aggregate motion and the particle relative position to the centre of gravity.

The inter-particle contacts of the final compact particle assemblies have a small initial overlap, this overlap may be reduced to a minimum value but it cannot be reduced to zero unless the particle radius is reduced so a single particle no longer interacts with others. In Potyondy and Cundall (2004), these initial forces are considered as normal forces prior to the start of the fracture test. In this work, an initial particle overlap is adopted on all particle assemblies, for this reason prior to the start of the simulation there are no inter-particle forces and the particle are only considered to interact if the particle overlap is higher that the initial recorded value. Only accounted, and in an incrementally way are the inter-particle forces which arise due to the inter-particle incremental relative displacement. By setting an initial particle overlap one reduces the geometric constraint in order to have more inter-particle contacts on each particle.

As shown in Fig. 7, either circular aggregate or polygonal aggregate are represented with circular particles clusters. For this reason it is only required to have simple circular particle interaction procedures even if more complexes shapes are present.

As will be shown here, the particle configuration is also a model parameter which needs to be taken into consideration. Here is referred a particle generation procedure that generates a compact particle assemblies that represents aggregate particles as a rigid cluster of circular particles and the space in between the aggregates is represented also with circular particles of smaller size. When compared to other models that only represent the contact between aggregate particles, Bazant *et al.* (1990) and Cusatis *et al.* (2003), a model that also represents the outer boundary with smaller particles has advantages if one is concerned with shear interaction between cracked surfaces.

4. Fracture tests

Table 2 presents the micro-properties that need to be defined in the particle model. The particle assemblies here defined have the aggregate content defined in Table 1, and are generated in a

Table 2 Micro elastic and strength properties

	E_c [GPa]	ν_s	σ_t^c [MPa]	C^c [MPa]	μ^c	G_{ji}^c [N/m]	G_{ji}^c [N/m]		E_c [GPa]	ν_s	σ_t^c [MPa]	C^c [MPa]	μ^c	G_{ji}^c [N/m]	G_{ji}^c [N/m]
AM	25.0	0.40	3.75	12.5	0.20	7.0	900.0	AM	70.0	0.40	3.25	9.75	0.20	5.0	900.0
MM	25.0	0.40	3.75	12.5	0.20	7.0	900.0	MM	15.0	0.40	6.50	19.5	0.20	10.0	900.0

(a) Uniform approach

(b) Heterogeneous approach

similar way to the particle assemblies created in the previous section.

The elastic constants are defined based on the Young's modulus E_c and Poisson's ratio ν_c of the contact equivalent continuum material. The contact stiffnesses are defined based on Eq. (6).

The particles that are used to represent an aggregate particle are considered to be aggregate particles and the particles that are used to set a final compact assembly are called matrix particles. Two different approaches are followed. In one approach the same micro-properties are adopted for all the inter-particle contacts regardless of its origin, the **uniform** approach. On the second approach different micro-properties are adopted for the inter-particle contacts between the aggregate and the matrix particles, **AM**, and for the inter-particle contacts between matrix particles, **MM**, the **heterogeneous** approach. In a 3D model and at this scale of analysis, concrete should be regarded as a three-phase material, for this reason different properties should be assigned to the particles and contacts representing the matrix, the aggregate and the interface zone, which is considered to be the weakest link in concrete. The **heterogeneous** approach has then a real physical meaning in a 3D model. In a 2D simulation the **heterogeneous** approach can be questioned, as the modelled layer of concrete should reflect the average properties of concrete over its depth. Both approaches are evaluated given the fact that the particle model under scrutiny is 2D.

The macroscopic values of the Young's modulus and Poisson's ratio are numerically determined in uniaxial tension and compression tests in particle assemblies with a rectangular geometry of 100 by 100 mm assuming plane stress constitutive equations. The contact strength properties need to be previously calibrated in uniaxial tension and compression tests. A given value for the softening energy is adopted for the normal direction of the contact G_{ft} and for the contact shear direction G_{fc} .

In Table 2 are presented the strength properties that give the best agreement in terms of the peak values of stress and fracture toughness. Table 3 presents the macroscopic numerical values that were obtained for the several particle systems here discussed in uniaxial tension and uniaxial compression.

The uniaxial tension tests are performed on particle assemblies with a rectangular geometry of 50 by 100 mm, while the uniaxial compression tests are performed for particle assemblies with a rectangular geometry of 100 by 100 mm. The load is applied to the particle assembly by setting the displacements of a rigid wall, Itasca (1995).

In the fracture tests here discussed there is no transmission of shear forces at the interface connecting the particle assembly to the rigid wall modelling the loading plate. Three types of particle systems are analysed: circular particle assemblies, **Circ.**, polygonal particle assemblies with a variable 1 to 2 aspect ratio, **Pol. 1-2**, and finally polygonal particle assemblies with a variable 2 to 3 aspect ratio, **Pol. 2-3**. The three particle assembly types have in common the aggregate quantity, the micro-properties and the aggregate surface roughness. In this work the aggregate surface

Table 3 Macro elastic and strength properties/numerical

	E [GPa]	σ_t [MPa]	σ_c [MPa]	G_f [N/m]		E [GPa]	σ_t [MPa]	σ_c [MPa]	G_f [N/m]
Circ.	32.0	3.71	38.7	45.5	Circ.	34.0	3.62	36.6	46.8
Pol. 1-2	34.0	3.70	36.0	47.0	Pol. 1-2	35.0	3.70	35.9	57.5
Pol. 2-3	34.0	3.50	34.8	47.6	Pol. 2-3	34.0	3.60	35.6	45.6
(a) Uniform approach					(b) Heterogeneous approach				

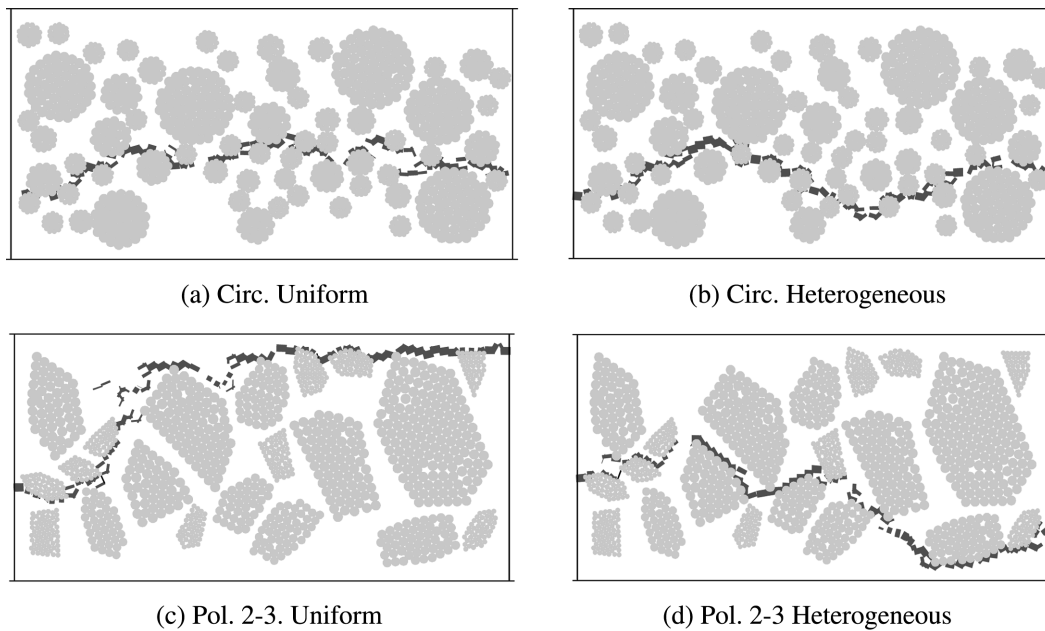


Fig. 8 Tensile tests – Final crack pattern

roughness is given by the average particle size used to discretize the interior of each aggregate particle.

Table 3 presents the macro-properties that have been numerically calculated with the particle model, namely the Young's modulus, the Poisson's coefficient ν , the ultimate tensile stress, the ultimate compression stress and the fracture energy which is given by the area of the stress-strain curve under tensile loading. From Table 3 it can be seen that the three particle systems here studied give similar results in both approaches, except for the tensile fracture energy. Table 3 shows that the particle assemblies of the type Pol. 1-2 lead to a higher fracture energy in the heterogeneous approach.

In Fig. 8 is shown the final crack patterns for two types of particle assemblies and for both approaches. The tensile load is induced in the particle assembly by moving upward the upper loading boundary, displacement control, which is not allowed to rotate. In general, the initial crack was occurring on the lateral zones of the particle assembly, the initial cracks were then propagating towards each other to the interior. At the end of the tensile test a final crack crossing the particle assembly is formed. In the heterogeneous approach the crack initiates at the weaker interface, which is the interface between the aggregate and the matrix particle. A similar behaviour is known to occur in concrete.

In the compression tests, where the load was applied in a displacement control fashion by incrementally displacing the upper boundary inwards, the particle assemblies were divided in a variable number of triangular/conical pieces that can shear off, Fig. 9. The macroscopic shear cracks are formed by an array of splitting cracks.

Even though the particle model includes a perfect friction contact model, pure friction forces on cracked contacts either do not occur or when occurring transmit a low value of contact force when compared with the contact forces present in the assembly.

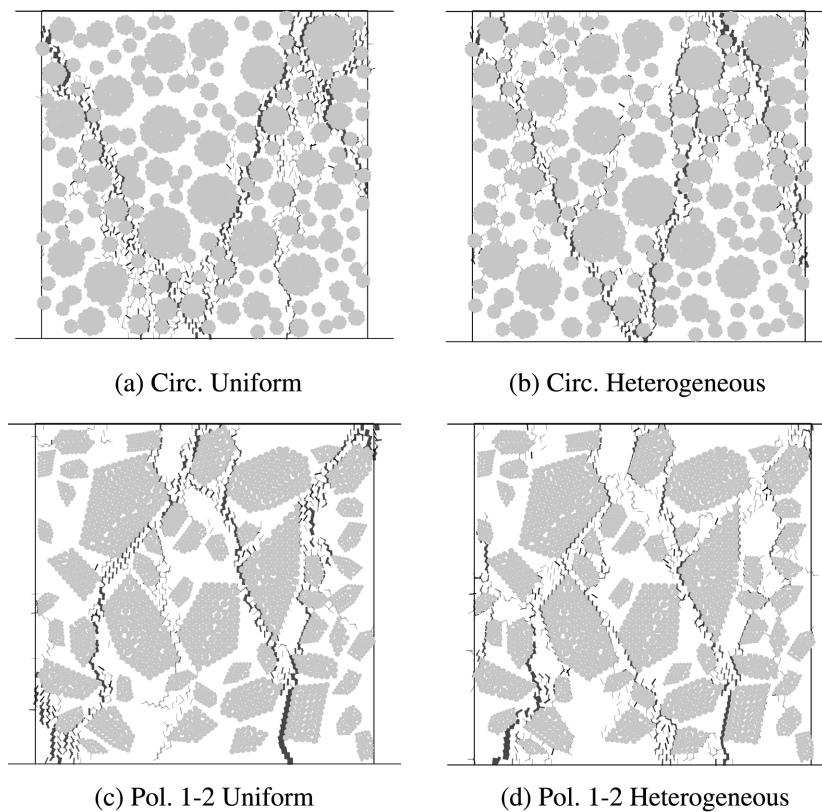


Fig. 9 Compression tests – Final crack pattern

In the particle model here adopted, the cracks can only propagate along the boundaries of the macro-particles modelling the aggregate and along the boundaries of the single rigid particles modelling the matrix, this fact explains a certain tortuosity of the final crack pattern. A similar mechanism is observed in concrete. As shown in Figs. 7 and 8, the particle model has the ability to follow the distinct fracture mechanisms known to occur in concrete for both uniaxial tension and uniaxial compression.

In Fig. 10 the stress/deformation diagrams numerically obtained are compared with the numerical results of Vonk (1993) which are known to compare well with concrete data. Fig. 10 shows that the tensile stress/deformation diagrams have a long tail. This phenomenon occurs even in the cases where an almost stress free macro-crack is formed. This long tail can be explained by the fact that active bridging contacts can still transmit the load through the particle assembly.

From Fig. 10 it is possible to verify that the geometry and the aspect ratio of the aggregate particle do not have a significant influence in the stress/deformation relationship in tension for the Uniform approach. Figs. 10(c) and 10(d) show that the non-circular particle shapes have a higher post-peak ductility.

From the analyses of Figs. 10 and 11 it is possible to conclude that the obtained numerical values are more brittle when compared to the numerical results obtained by Vonk (1993), namely the compression tests. It is also shown that the Heterogeneous approach leads to a more ductile response both in tension and compression. The more brittle values obtained with the particle model

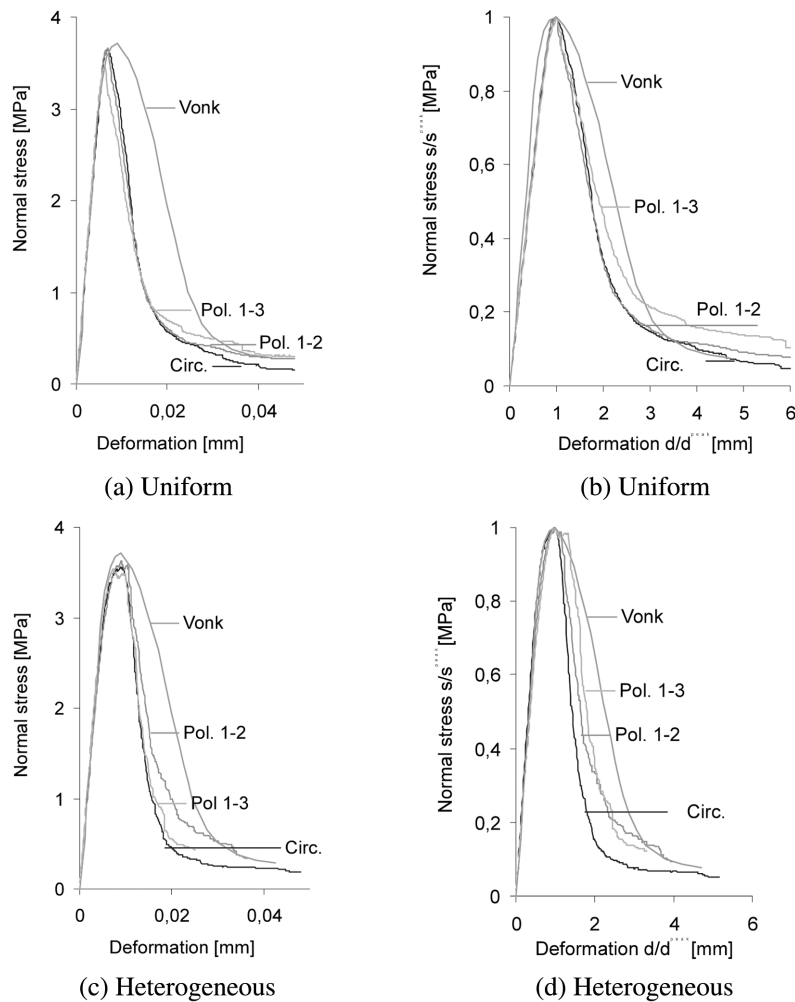


Fig. 10 Stress/deformation relationships – Tensile tests

can be partially explained by the fact that Vonk (1993) adopted an assembly of deformable polygonal particles for both the particles representing the aggregate and for the particles representing the cement matrix with a higher variation of contact strength.

From Fig. 10 it is possible to conclude that the three types of particles assemblies here studied have for the Uniform approach a similar response in compression. As shown in Fig. 10(b) the non-circular aggregate particles in the Heterogeneous approach lead to a relatively higher post-peak ductility. From Figs. 8 to 11 and Table 3, it is verified that it is possible to calibrate the particle model parameters in order to obtain a macro-response similar to the obtained in concrete. It can also be concluded that particle assemblies with non-circular aggregate shape have a softening behaviour similar to the softening occurring in particle assemblies with circular aggregates for both uniaxial tension and compression when using a Uniform approach. When adopting the Heterogeneous approach it can be seen that the assemblies with non-circular aggregate shape have a more ductile behaviour both in tension and compression. From the analyses of Figs. 9(d) and 10(b) it can be

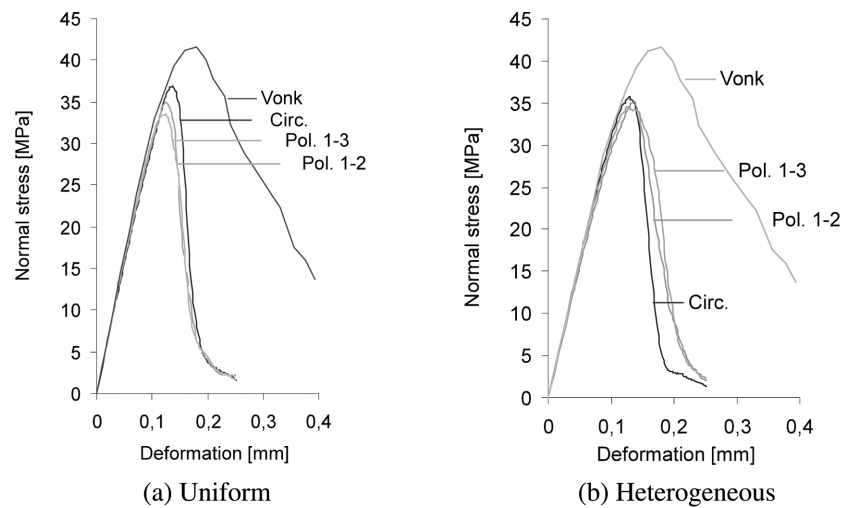


Fig. 11 Stress/deformation relationships – Compression tests

verified that in the Heterogeneous approach non-circular particle assemblies with different particle aspect ratio lead to similar results.

5. Conclusions

A particle model is presented that captures the fracture mechanisms by taking into consideration the concrete aggregate structure and the physical mechanisms related to the contact interaction. The particle model is shown to give figures of rupture similar to the obtained in concrete for similar fracture tests.

It is possible to calibrate the micro-properties of the particle model in order to obtain a macro-response similar to the observed for concrete. The calibration procedure needs to be executed for traditional fracture tests prior to the application of the model to other structural systems. The particle model is shown to capture the distinct fracture mechanisms known to occur in concrete under uniaxial tension and compression.

The particles representing the concrete aggregate should have a shape and an aspect ratio closer to the concrete aggregate shape and the concrete aggregate aspect ratio of the concrete to be modelled. For this reason it is important to devise flexible particle generation schemes.

When compared to the particle model adopted by Vonk (1993) the particle model here adopted is shown to be more brittle. Kotsovos (1983) through uniaxial compression tests in concrete cylinders verified that when there is no shear force transfer at the interface between the loading plates and concrete, the concrete has an immediate loss of loading capability as soon as the peak load is reached. The numerical results here obtained are in agreement with the experimental results obtained by Kotsovos (1983).

Particle assemblies with non-circular particles representing the aggregate and particle assemblies with circular particles representing the aggregate have a similar behaviour when adopting a Uniform approach. It is also shown that when adopting the Heterogeneous approach the non-circular particles

lead to an increase in the post-peak ductility both in tension and in compression. This can be partially explained by the fact that in the Heterogeneous approach the crack always initiates at the weaker interfaces, and as the circular assemblies have a higher number of particles the weaker interfaces are closer to each other making easier the process of crack propagation, compare Figs. 9(a) and 9(b) with Figs. 9(c) and 9(d) for the compression test. It should be noted that all the particle assemblies types here tested have a similar aggregate content and similar micro-properties.

In order to increase the fracture toughness of the particle assemblies it is possible to generate aggregate particles with a higher surface roughness. In Monteiro Azevedo (2003) it is shown that particle assemblies with aggregates having a higher surface roughness lead to an increase in the fracture toughness.

It would also be relevant to develop generation schemes that allowed the definition of polygonal shaped particles in the outer zone corresponding to the cement paste instead of circular particles as used in this study. This would create a higher variation of strength and stiffness in the particle assembly possibly leading to higher fracture toughness.

Acknowledgments

This work was partially carried out in the framework of the research project “POCI/ECM/56694/2004”, sponsored by the Portuguese Foundation for the Science and Technology (FCT).

References

- Bazant, Z. (1986), “Mechanics of distributed cracking”, *Appl. Mech. Rev.*, ASME, **4**(5), 675-705.
- Bazant, Z., Tabbara, M., Kazemi, M. and Cabot, G. (1990), “Random particle model for the fracture of aggregate or fiber composites”, *J. Eng. Mech.*, ASCE, **116**(8), 1686-1705.
- Cundall, P. and Strack, O. (1979), “A discrete numerical model for granular assemblies”, *Geotechnique*, **29**(1), 47-65.
- Cundall, P. (1980), “UDEC a generalized distinct element program for modelling jointed rock”, Final Tech. Rep. Eur. Res. Office (US Army Contract DAJA37-79-C-0548); NTIS order No. AD-A087 610/2.
- Cundall, P.A. and Hart, R.D. (1992), “Numerical modelling of discontinua”, *Eng. Computations*, **9**, 101-113.
- Cusatis, P., Bazant, Z. and Cedolin, L. (2003), “Confinement-shear lattice model for concrete damage in tension and compression: I. Theory”, *J. Eng. Mech.*, **129**(12), 1439-1448.
- Hentz, S., Daudeville, L. and Donzé, V. (2004), “Identification and validation of a discrete element model for concrete”, *J. Eng. Mech.*, **130**(6), 709-719.
- Herrmann, H. and Roux, S. (1989), “Modelization of fracture in disordered systems”, in *Statistical Models for the Fracture of Disordered Media* (Eds. H. Herrmann and S. Roux), 159-188, New York, North-Holland.
- Hrennikoff, A. (1941), “Solutions of problems of elasticity by the framework method”, *J. Appl. Mech.*, December.
- Itasca (1995), *PFC2D Particle Flow Code in 2 Dimensions* (Version 1.1 ed.), Itasca Consulting Group, Inc.
- Jensen, R.P., Bosscher, P., Plesha, M. and Edil, T. (1999), “DEM simulation of granular media - structure interface: Effects of surface roughness and particle shape”, *Int. J. Numer. Anal. Meth. Geomech.*, **23**, 531-547.
- Kotsovos, M. (1983), “Effect of testing techniques on the post-ultimate behaviour of concrete on compression”, *Material and Structures*, RILEM, **16**(91), 3-12.
- Meguro, K. and Hakuno, M. (1989), “Fracture analysis of concrete structures by the modified distinct element method”, *Struct. Eng. / Earthq. Eng.*, **6**(2), 283-294.
- Monteiro Azevedo, N., May, I. and Lemos, V. (2003), “Numerical simulations of plain concrete under shear

- loading conditions”, In H. Konietzky (Ed.), *Numerical Modeling in Micromechanics via Particle Methods*, Balkema, 79-86.
- Monteiro Azevedo, N. (2003), “A rigid particle discrete element model for the fracture analysis of plain and reinforced concrete”, PhD Thesis, Heriot-Watt University, Scotland.
- Monteiro Azevedo, N. and Lemos, V. (2004), “Generation of random particle assemblies for fracture studies of concrete”, 1-50, LNEC.
- Potyondy, D. and Cundall, P.A. (1996), “Modeling rock using bonded assemblies of circular particles”, *Proc. 2nd North American Rock Mechanics Symposium*, eds. Aubertin *et al.*, 1937-1944.
- Potyondy, D.O. and Cundall, P.A. (2004), “A bonded-particle model for rock”, *Int. J. Rock Mech. Min. Sci.*, **41**, 1329-1364.
- Rokugo, K. (1989), “Testing method to determine tensile softening curve and fracture energy of concrete”, *Fracture Toughness and Fracture Energy*, Balkema, 153-163.
- Sakaguchi, H. and Muhlhaus, H.-B. (1997), “Mesh free modelling of failure and localization in brittle materials, in deformation and progressive failure in geomechanics”, *Proc. IS-Nagoya 97*, Pergamon, Eds. A. Asaoka, T. Adachi and F. Oka, 15-21.
- Schlangen, E. and Garboczi, E. (1996), “New method for simulating fracture using an elastically uniform random geometry lattice”, *Int. J. Engng Sci.*, **34**(10), 1131-1144.
- Takada, S. and Hassani, N. (1996), “Analysis of compression failure of reinforced concrete by the modified distinct element method”, C.B. GD Manolis, DE Beskos (Ed.), *Advances in Earthquake Engineering, Earthquake Resistant Engineering Structures*. Comp. Mech. Publications.
- Underwood, P. (1983), *Dynamic Relaxation, in Computational Methods for Transient Analysis*, New Work:North-Holland, eds. T. Belytschko and T. Hughes, 246-265.
- Vonk, R. (1993), “A micromechanical investigation of softening of concrete loaded in compression”, *Heron*, **38**(3), 1-94.
- Wang, Z., Kwan, A. and Chan, H. (1999), “Mesoscopy study of concrete I: Generation of random aggregate structure and finite element mesh”, *Comput. Struct.*, **70**, 533-544.